

Phase coexistence in $\text{Bi}_{1-x}\text{Pr}_x\text{FeO}_3$ ceramics

D. V. Karpinsky^{1,2*}, I. O. Troyanchuk², V. Sikolenko^{3,4}, V. Efimov⁴, E. Efimova⁴, M. Willinger⁵, A.N. Salak¹, and A. L. Kholkin^{1,6}

¹ CICECO & Department of Materials and Ceramics Engineering, University of Aveiro, 3810-193 Aveiro, Portugal

² Scientific-Practical Materials Research Centre of NAS of Belarus, P. Brovka str. 19, 220072 Minsk, Belarus

³ Karlsruhe Institute of Technology, 76131 Karlsruhe, Germany

⁴ Joint Institute for Nuclear Research, 141980 Dubna, Russia

⁵ Fritz-Haber-Institut der Max-Planck-Gesellschaft, Abteilung Anorganische Chemie, Faradayweg 4-6, D-14195 Berlin, Germany

⁶ Ural Federal University, Lenin Ave. 51, Ekaterinburg 620083, Russia

Abstract

$\text{Bi}_{1-x}\text{Pr}_x\text{FeO}_3$ ceramics across the rhombohedral-orthorhombic phase boundary have been studied by X-ray diffraction, transmission electron microscopy and differential scanning calorimetry. The structural phase transitions in $\text{Bi}_{1-x}\text{Pr}_x\text{FeO}_3$ driven by doping concentration and temperature are significantly different from those in BiFeO_3 compounds doped with other rare-earth elements. The features of the structural transformations have been discussed based on the specific character of the chemical bonds associated with praseodymium ions. The detailed study of the crystal structure evolution clarified the ranges of both single phase and phase coexistence regions at different temperatures and dopant concentrations. For $x=0.125$ compound the three-phase coexistence region has been observed in the narrow temperatures range about 400 °C. The results explicate driving forces of the structural transitions and elucidate the origin of the remarkable physical properties of BiFeO_3 -based compounds near the morphotropic phase boundary.

Keywords: *Structure, Phase transformation, Phase diagram*

Introduction

Bismuth ferrite based multiferroics of the compositions near doping-induced phase boundary attract renewed interest in the last years due to their remarkable physical properties and fundamental physics involved [1-3]. It is assumed that the crystal structure of the BiFeO_3 compounds doped with the rare-earth elements (viz. $RE = La - Sm$) is characterized by the following phase transition sequence: polar rhombohedral – anti-polar orthorhombic – non-polar orthorhombic phases. In spite of a large number of studies the mechanism of the structural transitions in BiFeO_3 -based compounds near the morphotropic phase boundary (MPB) is still ambiguous and is the subject of the intensive discussions [3-7].

The most pronounced physical properties (viz. enhanced electromechanical response and remanent magnetization) were observed in BiFeO_3 doped with lanthanum and praseodymium near the polar rhombohedral (R) – anti-polar orthorhombic (O_2) phase boundary. The crystal structure of the $\text{Bi}_{1-x}(\text{La}, \text{Pr})_x\text{FeO}_3$ compounds within the $R - O_2$ phase boundary is characterized by the features specific either to La - or Pr - doping, viz. the incommensurately modulated crystal structure has been observed in the La -doped compounds [8, 9]. In addition, both La - and Pr -doped systems manifest isothermal structural transition [5, 10]. Temperature evolution of the crystal structure obtained for the Pr -doped compounds differs significantly from that of the

* Corresponding author. Tel.: +351 234401464; Mob. +351 961544399; e-mail: karpinski@ua.pt

compounds doped with other rare-earth ions. The most intriguing feature of the $\text{Bi}_{1-x}\text{Pr}_x\text{FeO}_3$ crystal structure has been observed near the transition to the non-polar orthorhombic phase where the coexistence of the rhombohedral and both orthorhombic phases has been suggested [10-12].

The present study is aimed at further clarification of the crystal structure of $\text{Bi}_{1-x}\text{Pr}_x\text{FeO}_3$ ceramics within the morphotropic phase boundary region. In this work, thermal phase stability and driving forces for temperature-induced structural transitions are investigated. The study is focused on the temperature evolution of the crystal structure of *Pr*-doped BiFeO_3 ceramics characterized by the coexistence of the structural phases at room temperature. Understanding the exact crystal structure of BiFeO_3 -based compounds at the phase boundary and the factors determining structural stability of the compounds near the MPB are of fundamental interest and will bring forward practical perspectives of using functional materials with controlled physical properties.

Experimental

Ceramic samples of $\text{Bi}_{1-x}\text{Pr}_x\text{FeO}_3$ (molar concentrations 0.11, 0.125, and 0.15) were prepared by the two-stage solid-state reaction technique [10]. High-purity oxides taken in a stoichiometric ratio were thoroughly mixed using a planetary ball mill (Retsch PM 200). The ceramics were synthesized at 930 – 1030°C (synthesis temperature was increased with the dopant concentration) followed by a fast cooling down to room temperature. X-ray diffraction measurements were performed with a Rigaku D/MAX-B diffractometer (Cu-K_α radiation) equipped with the Anton Paar heating stage. Diffraction data were analyzed by the Rietveld method using the FullProf software package [13]. Differential scanning calorimetry (DSC) was carried out with a Setaram SETSYS 16/18 instrument in a flowing air. High Resolution Transmission Electron Microscopy (HRTEM) measurements have been performed using a FEI TITAN 80-300 microscope.

Results and discussion

Concentration- and temperature-induced transitions

X-ray diffraction data of the $\text{Bi}_{1-x}\text{Pr}_x\text{FeO}_3$ compounds recorded at room temperature testify that the polar rhombohedral and the anti-polar orthorhombic phases coexist in the concentration range $0.11 \leq x \leq 0.15$. The crystal structure of $\text{Bi}_{0.89}\text{Pr}_{0.11}\text{FeO}_3$ compound at room temperature has been successfully refined assuming 90% of the rhombohedral phase (*R*-phase, space group *R3c*) and 10% of the orthorhombic phase (*O*₂-phase). The rhombohedral phase is the same as observed in $\text{Bi}_{1-x}\text{Pr}_x\text{FeO}_3$ compounds with lower dopant concentration $x < 0.11$ [10, 14]. The orthorhombic phase has been refined using *Pnam* space group with a lattice metric $\sqrt{2}a_p * 2\sqrt{2}a_p * 4a_p$ (a_p is the fundamental perovskite lattice parameter). In the orthorhombic lattice the ions residing at *A*- and/or *B* perovskite positions are shifted along the *b*-axis in opposite directions thus forming an anti-polar order, similar to that observed in PbZrO_3 [9, 15]. Praseodymium doping apparently leads to the increase of the orthorhombic phase fraction, the amount of the rhombohedral phase proportionally being decreased. The $x=0.125$ compound contains 25% of the orthorhombic phase, whereas for the $x=0.15$ compound the *O*₂-phase is the dominant one and the amount of the rhombohedral phase is about 10% at room temperature.

Structural analysis of the $\text{Bi}_{1-x}\text{Pr}_x\text{FeO}_3$ compounds across the phase boundary has been performed considering the phenomenon of isothermal structural transition observed in the RE-doped BiFeO_3 ceramics [5]. The diffraction data discussed in in this work have been obtained for the compounds left at room temperature for at least two months after synthesis, thus the crystal structure of the ceramics is supposed to be fully relaxed.

We have focused structural investigations on the temperature evolution of $\text{Bi}_{0.875}\text{Pr}_{0.125}\text{FeO}_3$ and $\text{Bi}_{0.85}\text{Pr}_{0.15}\text{FeO}_3$ compounds the crystal structure of these is characterized by the coexistence of the R - and O_2 - phases with the relative ratio ($R:O_2$) of 3:1 and 1:9, respectively, at room temperature. The temperature diffraction data obtained for the $x=0.125$ compound demonstrate gradual decrease of the amount of the orthorhombic phase with temperature, whereas the fraction of the rhombohedral phase proportionally increases.

The analysis of the XRD temperature data testifies progressive increase of the lattice parameters of the $x=0.125$ compound up to 350 °C whereas the diffraction peaks specific for the quadrupled c -parameter become negligible at about 150 °C. Above this temperature the orthorhombic phase of the compound can be successfully described using $Pbam$ space group with $\sqrt{2}a_p * 2\sqrt{2}a_p * 2a_p$ metric specific to the crystal structure of $\text{Bi}_{1-x}\text{Pr}_x\text{FeO}_3$ compounds at room temperature with doping concentration $x > 0.25$ [10, 14]. The amount of the orthorhombic phase gradually decreases with temperature and its fraction amounts to about 15% at 350 °C. Above this temperature the orthorhombic phase further diminishes while the new orthorhombic phase (O_1) appears and can be successfully refined using a centrosymmetric $Pnma$ space group. In the narrow temperature range around 390 °C the coexistence of three structural phases (R , O_2 , O_1) has been verified thus confirming the idea proposed in the previous study [16]. The coexistence of the three structural phases at elevated temperatures has been confirmed by thermal HRTEM images (Fig. 1). Three structural phases can be distinctively observed within one crystal grain with the size of about 40 nm. The analysis of the FFT images obtained from the appropriate structural regions attested the coexistence of structural phases estimated from the X-ray diffraction data. The HRTEM images obtained at different temperatures allowed to estimate temperature evolution of the mentioned structural phases, in particular lattice dynamics of the structural transformations in the $x=0.125$ compound. These data will be published elsewhere. The temperature region of the three phase coexistence state estimated from the HRTEM data (300 – 500 °C) is significantly wider than that calculated based on the X-ray diffraction data and it can be explained by the local character of TEM measurements.

The evolution of the crystal structure across the three-phase coexistence region is thoroughly analyzed and presented in the next section. The anti-polar orthorhombic phase disappears slightly above 400 °C while the amount of newly appeared non-polar orthorhombic phase rapidly increases. The unit cell parameters attributed to the rhombohedral and the non-polar orthorhombic structural phases gradually increase with temperature up to about 550 °C. Above this temperature the rhombohedral phase vanishes and the single phase state with non-polar orthorhombic structure stabilizes (Fig. 2).

Temperature evolution of the crystal structure calculated for the $\text{Bi}_{0.85}\text{Pr}_{0.15}\text{FeO}_3$ compound has significantly different behavior. The fraction of the rhombohedral phase estimated for the compound (about 10% at room temperature) continuously decreases with temperature. Above 100 °C we could not detect any traces of the rhombohedral phase and the crystal structure can be considered as a single phase orthorhombic one up to 350°C. The XRD pattern recorded at 350°C reveals new diffraction peaks with negligibly small intensity. These peaks were

successfully refined within $\sqrt{2a_p} * 2a_p * \sqrt{2a_p}$ metric and prove the emergence of the new non-polar orthorhombic phase (Fig. 3).

The diffraction peaks attributed to the anti-polar phase disappear above 400 °C and the structural transformation to the non-polar phase is considered to occur within the temperature range 350 – 400°C. While careful analysis of the diffraction patterns reveals certain asymmetry of the peaks above 400°C which attests the presence of the anti-polar orthorhombic phase in the compound up to 450°C. Above this temperature the crystal structure is considered to be single phase orthorhombic one and can be described using orthorhombic *Pnma* space group. It should be noted that the quadrupling of the *c*-parameter in the anti-polar phase remains up to the temperature of the structural transition to the non-polar orthorhombic phase, while in $\text{Bi}_{0.875}\text{Pr}_{0.125}\text{FeO}_3$ compound it disappears around 150°C.

Three -phase coexistence region

In order to clarify the structural peculiarities of the three-phase coexistence state observed for the $x=0.125$ compound we analyzed the temperature evolution of the crystal structure of the $x=0.125$ and 0.15 compounds in the temperature range 300 – 600 °C. In the temperature ranges of the expected structural transitions the XRD patterns were recorded at 10 °C steps.

In the temperature range of 380 – 410°C which has been estimated as the three-phase coexistence region for the $x=0.125$ compound, the unit cell parameters attributed to both orthorhombic phases quickly change (Fig. 4). Within the mentioned temperature interval the *b*-parameter of the anti-polar orthorhombic phase reduces by about 0.5%, the *c*-parameter notably increases (0.2%), whereas the *a*-parameter slightly increases; thus the volume of the anti-polar unit cell is decreased by 0.3% in this temperature range. It should be noted that reduction of the *b*-parameter is apparently associated with a decrease of the anti-polar displacement of the ions along the *b*-axis of the orthorhombic lattice. The anti-polar displacement is associated with $b/2a$ ratio which gradually decreases with temperature down to unity at about 410 °C.

In the temperature interval 380 – 410 °C the unit cell parameters of the non-polar orthorhombic phase change quite slowly. The *b*-parameter slightly increases, the *c*-parameter shows an opposite trend and decreases by about 0.3%, the *a*-parameter demonstrates only small decrease, thus the related unit cell volume remains nearly constant. The lattice parameters of the rhombohedral phase gradually increase in the temperature range 380 – 410 °C and the *R*-phase unit cell slightly expands.

Analysis of the structural evolution of the anti-polar and the non-polar orthorhombic phases within the three-phase region in the $x=0.125$ compound permitted to clarify the mechanism of the phase transition in the *Pr*-doped BiFeO_3 ceramics. It was mentioned that the XRD data for the $x=0.125$ compound testify gradual reduction of the anti-polar order with temperature increase and its disruption ends up at about 410 °C. The transformation from the anti-polar structure to the non-polar one is accompanied by a modification of the unit cell lattice wherein the *b*-parameter (indicative for the anti-polar order) in O_2 -phase is decreased by two times and its value becomes close to the *c*-parameter in the O_1 -phase. The *c*-parameter in the O_2 -phase demonstrates opposite trend and rapidly increases in the temperature range 390 – 410 °C becoming close to the *b*-parameter of the O_1 -phase. The *a*-parameter of the O_2 -phase remains nearly constant within the above mentioned temperature range and its value is almost equal to the *a*-parameter of the O_1 -phase.

Considering the described structural changes the most probable scenario of the phase transition assumes a *transformation* of the anti-polar structure into the non-polar one associated

with a decrease of the unit cell volume of about 1%. This transformation is in accordance with the group-subgroup relation between the appropriate space groups *Pbam* (#55) and *Pnma* (#62). Taking into account the number of formula units per primitive unit cell for these space groups (8 and 4 for *Pbam* and *Pnma*, correspondingly) and the equality of the orders of the related point groups one can consider one step transformation *Pbam* → *Pnma* with the transformation index $i = 2$.

The difference between the temperature-induced structural transitions in the $x=0.125$ and $x=0.15$ compounds

It should be noted that the structural transformation into the non-polar orthorhombic state observed in the *Pr*-doped compounds is significantly different from those attested for BiFeO_3 compounds doped with other rare-earth elements [10-12, 17]. In the *La*-doped compound with similar phase ratio (at room temperature), the above-mentioned structural transition occurs via formation of the single phase state with rhombohedral symmetry [9, 10, 16]. Different character of the structural transition observed in the *La*- and *Pr*-doped compounds is confirmed by DTA/TG measurements [9, 16, 18] which testify the absence of any distinct anomaly in the *Pr*-doped compounds as compared with analogous *La*-doped BiFeO_3 compounds. Taking into account the DTA/TG and diffraction data available for the *La*- and *Pr*-doped compounds one may suggest that it is the specific character of the *Pr* – O chemical bonds that determines distinctive structural transition in the $\text{Bi}_{0.875}\text{Pr}_{0.125}\text{FeO}_3$.

The analysis of the temperature evolution of the crystal structure testifies significantly different character of the structural transition to the non-polar orthorhombic phase occurred in the $x=0.125$ and $x=0.15$ compounds. In the temperature range 100 – 380 °C, i.e. below the transition temperature, the crystal structure of the $\text{Bi}_{0.85}\text{Pr}_{0.15}\text{FeO}_3$ compound has been successfully refined assuming single phase anti-polar orthorhombic structure. The transformation of the anti-polar orthorhombic phase can be described by the model proposed for the $x=0.125$ compound and the changes of the unit cell parameters calculated for the $x=0.15$ compound are similar to those estimated in $x=0.125$ compound. Within the temperature range of the phase transition the *b*- and *c*-parameters are decreased by ~0.15%, the *a*-parameter remains nearly constant and follows the trend observed in the $\text{Bi}_{0.875}\text{Pr}_{0.125}\text{FeO}_3$. The significant difference between the *b*-parameter of the O_2 -phase and the related *c*-parameter of the O_1 -phase (~2.5%) as well as between the *c*-parameter of the O_2 -phase and *b*-parameter of the O_1 -phase (~1.1%) resulted in the decrease of the orthorhombic unit cell volume of ~1.1% (Fig. 5) which is less than the change of the relevant unit cell volume in the $x=0.125$ compound (~1.9%).

The difference in the structural transition is confirmed by DSC data which testify notable anomaly at about 360 °C (Fig. 5d) unlike the $x=0.125$ compound (Fig. 4d). The anomaly at 360 °C is associated with the structural transformation from the anti-polar into the non-polar orthorhombic phase, while similar transition in $x=0.125$ compound occurs near 380 °C which is close to the magnetic transition temperature [10, 14]. The anomaly observed in the DSC curves of the $x=0.15$ compound is proportionally less pronounced than that in the $x=0.125$ one and correlates well with the estimated phase ratio. The structural transition from the polar rhombohedral into the non-polar orthorhombic phase occurs in $x=0.125$ compound about 440 °C (around this temperature the transition occurs much faster) and has smaller heat transfer as compared with the transition between the orthorhombic phases (Figs. 4d, 5d).

Comparing the crystal structure evolution of the $x=0.125$ and $x=0.15$ compounds one can deduce that the prevailing amount of the rhombohedral phase determines the formation of the

unique structural state where three structural phases coexist. The phase coexistence state is associated with increased mechanical compliance resulted in enhanced elastic and piezoelectric properties of the compounds as confirmed by the Piezoresponse Force Microscopy measurements in $\text{Bi}_{0.875}\text{Pr}_{0.125}\text{FeO}_3$ [14]. Enhanced electromechanical properties have also been detected in $\text{Bi}_{1-x}\text{RE}_x\text{FeO}_3$ compounds series ($\text{RE} = \text{La}, \text{Nd}, \text{Sm}$) for the compositions near the morphotropic phase boundary [5, 19] which verify the results of theoretical estimations [20, 21].

Conclusions

We studied temperature- and composition- driven structural transitions in $\text{Bi}_{1-x}\text{Pr}_x\text{FeO}_3$ ceramics with compositions within the phase boundary between the rhombohedral polar and orthorhombic anti-polar phases. Thermal diffraction data allowed delineating the single phase and phase coexistence regions. The three phase coexistence region has been confirmed in $\text{Bi}_{0.875}\text{Pr}_{0.125}\text{FeO}_3$ compound using both diffraction and TEM data. The specific character of the structural transitions occurred in the studied *Pr*-doped BiFeO_3 ceramics and, in particular, in the $x=0.125$ compound has been discussed assuming special character of the *Pr* – *O* chemical bonds and decisive role of the rhombohedral phase causing high mechanical compliance of the compounds near the phase transition. Low structural stability of the rhombohedral phase estimated for the $x=0.125$ compound with dominant rhombohedral phase results in the enhanced electromechanical properties of the ceramics near the phase boundary. The obtained results clarified the origin of driving forces of the structural phase transitions and define the phase coexistence conditions which may significantly improve physical properties of BiFeO_3 -based ceramic materials.

Acknowledgements

The authors would like to acknowledge the FCT (grant # SFRH/BPD/42506/2007) and RFFI (grant ***). The work at CICECO was partly supported by the FCT Grant Pest-C/CTM/LA0011/013. Dr^a Maria Celeste Azevedo is acknowledged for the DSC measurements.

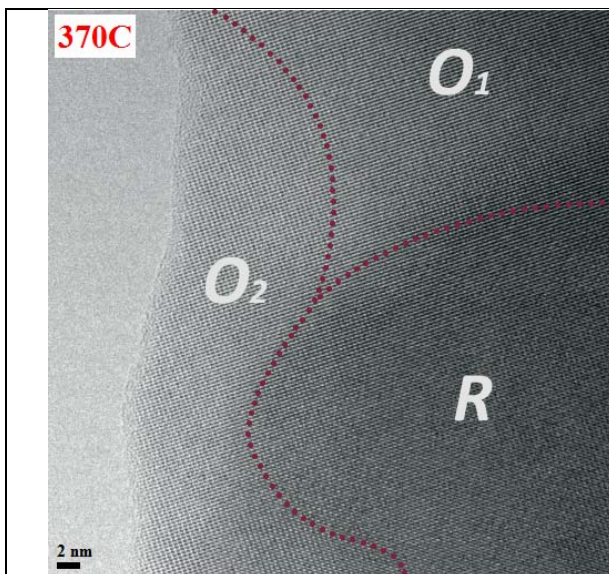


Figure 1. HRTEM image of the $x=0.125$ compound at $T=370$ C. The regions associated with different structural phases are delineated by dashed line.

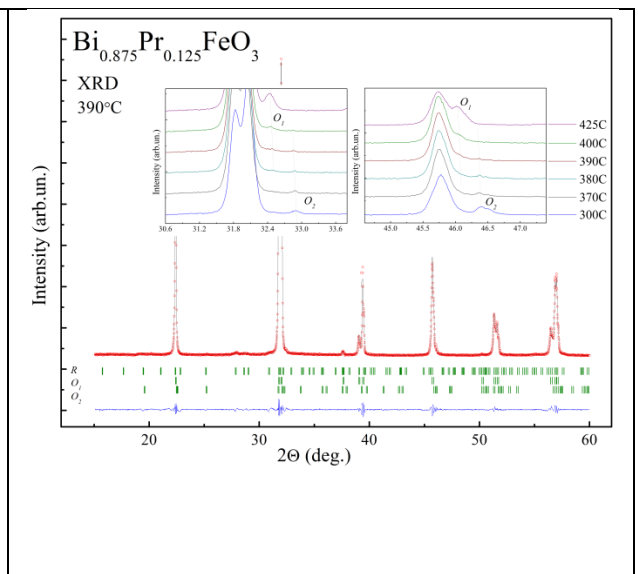


Figure 2. The XRD pattern of the $\text{Bi}_{0.875}\text{Pr}_{0.125}\text{FeO}_3$ compound at 390 °C (circles are experimental data, lines are calculated ones). Bragg positions are indicated

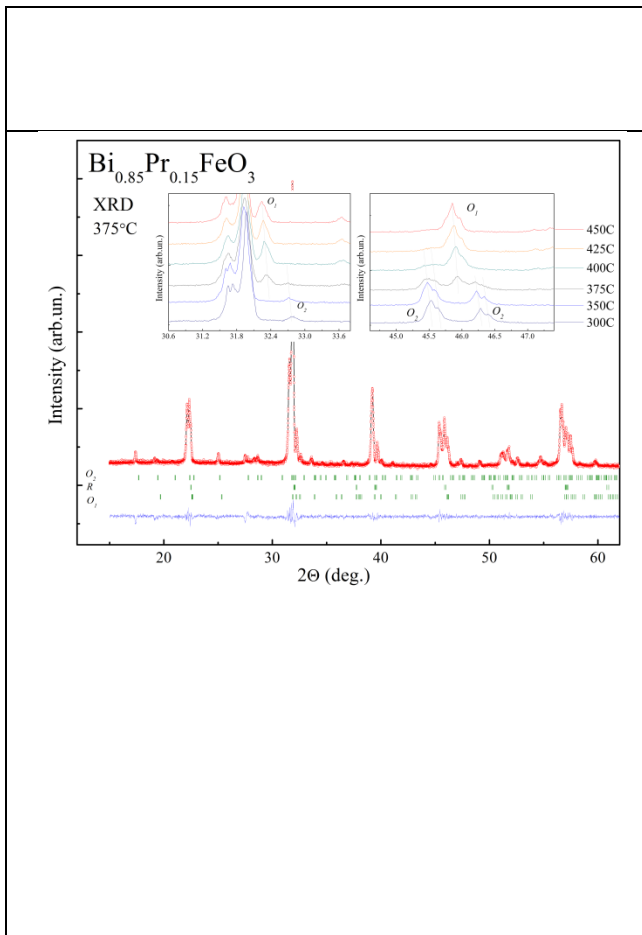


Figure 3. The XRD pattern of the $\text{Bi}_{0.85}\text{Pr}_{0.15}\text{FeO}_3$ compound at 375°C . Bragg positions are indicated by vertical ticks (the anti-polar orthorhombic phase, rhombohedral one and non-polar orthorhombic – from top to bottom). The insets show thermal evolution of the structural peaks specific for different phases.

by vertical ticks (the rhombohedral phase, non-polar orthorhombic, anti-polar orthorhombic – from top to bottom). The insets show thermal evolution of the structural peaks characteristic for O_2^- and O_1^- phases.

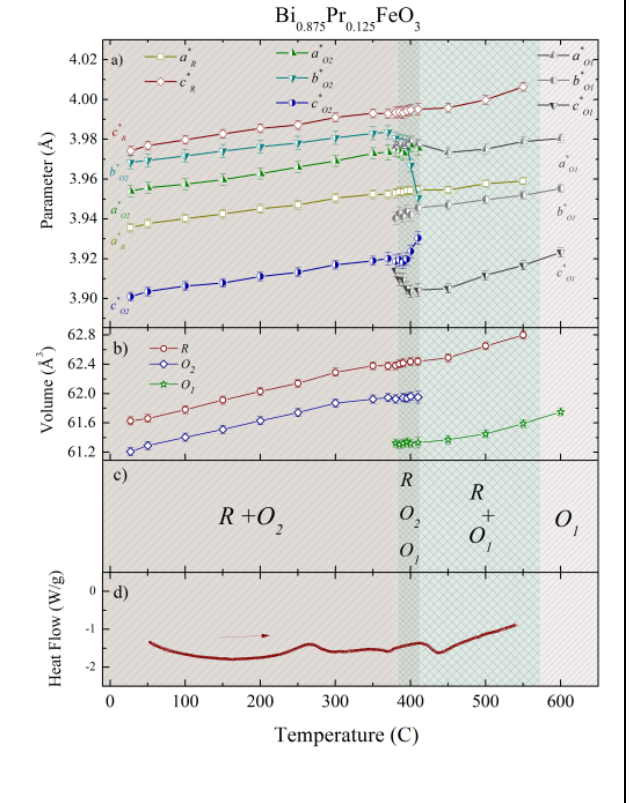


Figure 4. Temperature evolution of the structural phases and lattice parameters of the $\text{Bi}_{0.875}\text{Pr}_{0.125}\text{FeO}_3$ compound: a) unit cell parameters; b) unit cell volumes; c) structural phase diagram; d) DSC data of the compound.

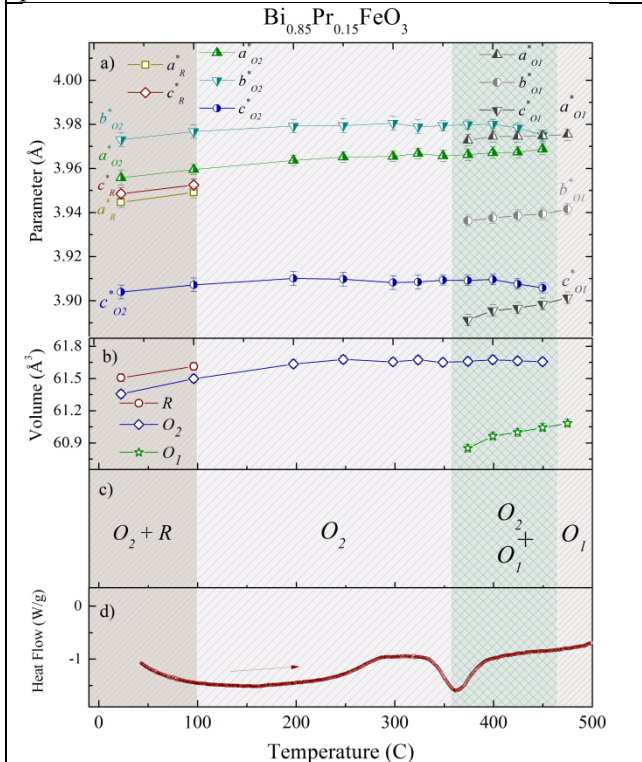


Figure 5. Temperature evolution of the structural phases and lattice parameters of the $\text{Bi}_{0.85}\text{Pr}_{0.15}\text{FeO}_3$ compound: a) unit cell parameters; b) unit cell volumes; c) structural phase diagram; d) DSC data of the compound.

Figure 5. Temperature evolution of the structural phases and lattice parameters of the $\text{Bi}_{0.85}\text{Pr}_{0.15}\text{FeO}_3$ compound: a) unit cell parameters; b) unit cell volumes; c) structural phase diagram; d) DSC data of the compound.

References

- [1] D. Kan, L. Palova, V. Anbusathaiah, C. J. Cheng, S. Fujino, V. Nagarajan, K. M. Rabe, I. Takeuchi (2010) *Adv. Funct. Mater.* 20: 1108
- [2] Y. H. Chu, Q. Zhan, C.-H. Yang, M. P. Cruz, L. W. Martin, T. Zhao, P. Yu, R. Ramesh, P. T. Joseph, I. N. Lin, W. Tian, D. G. Schlom (2008) *Appl. Phys. Lett.* 92: 102909
- [3] G. L. Yuan, S. W. Or, J. M. Liu, Z. G. Liu (2006) *Appl. Phys. Lett.* 89: 052905
- [4] X. Chen, G. Hu, W. Wu, C. Yang, Xi Wang, S. Fan (2010) *J. Am. Ceram. Soc.* 93: 948
- [5] I. O. Troyanchuk, D. V. Karpinsky, M. V. Bushinsky, et al. (2011) *Phys. Rev. B* 83: 054109
- [6] G. Le Bras, P. Bonville, D. Colson, A. Forget, N. Genand-Riondet, R. Tourbot (2011) *Physica B* 406: 1492
- [7] D. V. Karpinsky, I. O. Troyanchuk, J. V. Vidal, N. A. Sobolev, A. L. Kholkin (2011) *Solid State Commun.* 151: 536
- [8] D. V. Karpinsky, I. O. Troyanchuk, O. S. Mantyskaya, V. A. Khomchenko, A. L. Kholkin (2011) *Solid State Commun.* 151: 1686
- [9] D. A. Rusakov, A. M. Abakumov, K. Yamaura, A. A. Belik, G. Van Tendeloo, E. Takayama-Muromachi (2010) *Chem. Mater.* 23: 285
- [10] I. O. Troyanchuk, D. V. Karpinsky, M. V. Bushinsky, O. S. Mantyskaya, N. V. Tereshko, V. N. Shut (2011) *J. Am. Ceram. Soc.* 94: 4502
- [11] V. A. Khomchenko, J. A. Paixão, B. F. O. Costa, et al. (2011) *Cryst. Res. Technol.* 46: 238. Doi:10.1002/crat.201100040
- [12] V. A. Khomchenko, D. V. Karpinsky, A. L. Kholkin, et al. (2010) *J. Appl. Phys.* 108: 074109
- [13] J. Rodriguez-Carvajal (1993) *Physica B* 192: 55
- [14] V. A. Khomchenko, I. O. Troyanchuk, D. V. Karpinsky, J. A. Paixao (2012) *J. Mater. Sci.* 47: 1578
- [15] S. Teslic, and T. Egami (1998) *Acta Cryst. B* 54: 750
- [16] D. V. Karpinsky, I. O. Troyanchuk, M. Tovar, et al. (2014) *J. Am. Ceram. Soc.* to be published
- [17] I. Levin, M. G. Tucker, H. Wu, et al. (2011) *Chem. Mater.* 23: 2166
- [18] D. V. Karpinsky, I. O. Troyanchuk, M. Tovar, V. Sikolenko, V. Efimov, A. L. Kholkin (2013) *J. Alloys Compd.* 555: 101
- [19] D. V. Karpinsky, I. O. Troyanchuk, V. Sikolenko, V. Efimov, A. L. Kholkin (2013) *J. Appl. Phys.* 113: 187218
- [20] D. Damjanovic (2010) *Appl. Phys. Lett.* 97: 062906
- [21] O. E. González-Vázquez, J. C. Wojdeł, O. Diéguez, J. Íñiguez (2012) *Phys. Rev. B* 85: 064119